NASA/TM—2010-216769/PART2

GT2010–23386

Results of an Advanced Fan Stage Operating Over a Wide Range of Speed and Bypass Ratio
Part 2: Comparison of CFD and Experimental Results

Mark L. Celestina and Kenneth L. Suder
Glenn Research Center, Cleveland, Ohio

Sameer Kulkarni
Case Western Reserve University, Cleveland, Ohio

October 2010

NASA STI Program . . . in Profile

Since its founding, NASA has been dedicated to the advancement of aeronautics and space science. The NASA Scientific and Technical Information (STI) program plays a key part in helping NASA maintain this important role.

The NASA STI Program operates under the auspices of the Agency Chief Information Officer. It collects, organizes, provides for archiving, and disseminates NASA's STI. The NASA STI program provides access to the NASA Aeronautics and Space Database and its public interface, the NASA Technical Reports Server, thus providing one of the largest collections of aeronautical and space science STI in the world. Results are published in both non-NASA channels and by NASA in the NASA STI Report Series, which includes the following report types:

- TECHNICAL PUBLICATION. Reports of completed research or a major significant phase of research that present the results of NASA programs and include extensive data or theoretical analysis. Includes compilations of significant scientific and technical data and information deemed to be of continuing reference value. NASA counterpart of peer-reviewed formal professional papers but has less stringent limitations on manuscript length and extent of graphic presentations.

- TECHNICAL MEMORANDUM. Scientific and technical findings that are preliminary or of specialized interest, e.g., quick release reports, working papers, and bibliographies that contain minimal annotation. Does not contain extensive analysis.

- CONTRACTOR REPORT. Scientific and technical findings by NASA-sponsored contractors and grantees.

- CONFERENCE PUBLICATION. Collected papers from scientific and technical conferences, symposia, seminars, or other meetings sponsored or cosponsored by NASA.

- SPECIAL PUBLICATION. Scientific, technical, or historical information from NASA programs, projects, and missions, often concerned with subjects having substantial public interest.

- TECHNICAL TRANSLATION. English-language translations of foreign scientific and technical material pertinent to NASA's mission.

Specialized services also include creating custom thesauri, building customized databases, organizing and publishing research results.

For more information about the NASA STI program, see the following:

- Access the NASA STI program home page at *http://www.sti.nasa.gov*

- E-mail your question via the Internet to *help@ sti.nasa.gov*

- Fax your question to the NASA STI Help Desk at 443–757–5803

- Telephone the NASA STI Help Desk at 443–757–5802

- Write to:
  NASA Center for AeroSpace Information (CASI)
  7115 Standard Drive
  Hanover, MD 21076–1320

Results of an Advanced Fan Stage Operating Over a Wide Range of Speed and Bypass Ratio
Part 2: Comparison of CFD and Experimental Results

Mark L. Celestina and Kenneth L. Suder
Glenn Research Center, Cleveland, Ohio

Sameer Kulkarni
Case Western Reserve University, Cleveland, Ohio

National Aeronautics and
Space Administration

Glenn Research Center
Cleveland, Ohio 44135

October 2010

Acknowledgments

Level of Review: This material has been technically reviewed by technical management.

Available from

Results of an Advanced Fan Stage Operating
Over a Wide Range of Speed and Bypass Ratio
Part 2: Comparison of CFD and Experimental Results

Mark L. Celestina and Kenneth L. Suder
National Aeronautics and Space Administration
Glenn Research Center
Cleveland, Ohio 44135

Sameer Kulkarni
Case Western Reserve University
Cleveland, Ohio 44106

Abstract

NASA and GE teamed to design and build a 57 percent engine scaled fan stage for a Mach 4 variable cycle turbofan/ramjet engine for access to space with multipoint operations. This fan stage was tested in NASA's transonic compressor facility. The objectives of this test were to assess the aerodynamic and aero mechanic performance and operability characteristics of the fan stage over the entire range of engine operation including: 1) sea level static take-off; 2) transition over large swings in fan bypass ratio; 3) transition from turbofan to ramjet; and 4) fan wind-milling operation at high Mach flight conditions.

This paper will focus on an assessment of APNASA, a multistage turbomachinery analysis code developed by NASA, to predict the fan stage performance and operability over a wide range of speeds (37 to 100 percent) and bypass ratios.

Introduction

The research objectives were to assess the capability of state-of-the-art (SOA) design and analysis tools used for conventional subsonic turbomachinery to design and predict the performance and operability of an advanced fan stage designed to meet the requirements for the first stage of a two-stage-to-orbit hypersonic vehicle. The ultimate goal was to have confidence in the tools to design and analyze these advanced Turbine Based Combined Cycle (TBCC) configurations to meet future mission requirements. The metrics for the CFD analysis was to determine fan stage performance in terms of adiabatic efficiency (at a design pressure ratio and mass flow) and fan stage operability in terms of stall margin (over the operating line).

The approach taken to assess the SOA design and analysis tools was to: 1) design and predict the performance and operability of a relevant TBCC engine fan stage; 2) experimentally map the aerodynamic and aeromechanic performance and stability limits over the operating range; 3) compare measured results to pretest CFD predictions; and 4) assess the strengths and weaknesses of the SOA tools.

In this paper, we will describe the lessons learned in a pretest CFD analysis and results of comparing the post-test CFD analysis with experimental data then wrap-up with an overall comparison of the design with the CFD and experimental results. The CFD tool used in this paper is APNASA (Ref. 1).

Nomenclature

MF	Mass Flow
NS	Near Stall Point
OP	Operating Point
PR	Pressure Ratio
SM	Stall Margin
TR	Temperature Ratio

RTA Fan Rig

The GE57 fan rig was designed as a 57 percent linear scale of the proposed demonstrator engine. It was designed to demonstrate the feasibility of the high-pressure ratio fan across the required broad operating range. The fan diameter is 55.88 cm (22 in.) and at 100 percent speed develops a design pressure ratio of 2.46 at an inlet corrected flow rate of 37.19 kg/s (82 lbm/s). The stage adiabatic efficiency at this point was projected to be 85.7 percent and stall margin was projected to be 11 percent. The fan rotational speed at 100 percent speed is 17,280 rpm with a corresponding tip speed of about 506 m/s (1660 ft/s). A variable fan OGV was designed for this rig for high Mach flight conditions. Following the OGV is the split flowpath with struts that extend through both flowpaths. The lower path directs flow through the core of the engine and the upper path bypasses the core. Two liners over the rotor were used in the experiment, a grooved casing and a smooth casing. The CFD was only run for the smooth liner. For more details about the design, see (Ref. 2). For information on the instrumentation survey planes, see (Ref. 3).
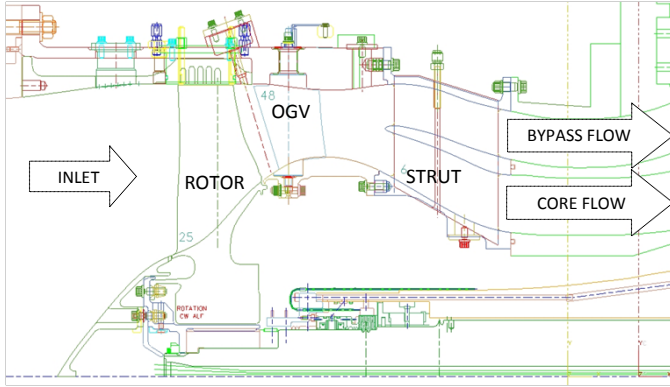
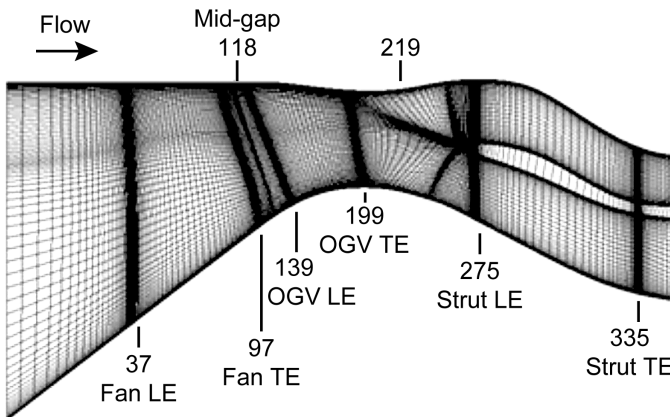Figure 1.—Fan stage components and flowpath.

Figure 2.—Axisymmetric view of simulation grid.

APNASA Code

APNASA is a multistage analysis code which provides the ability to analyze the complete fan stage consisting of the fan rotor, outlet guide vane (OGV), and splitter/strut mid-frame assembly (see Fig. 1). This approach is unique from 'typical' single passage codes that solve for one blade row at a time by systematically marching through the compression system blade row by blade row utilizing averaged or mixed-out solutions from the upstream blade row as input to the downstream blade row. APNASA solves for all blade rows under consideration which, in this case, includes the fan rotor, OGV and splitter/strut mid-frame assembly. The APNASA fan rotor solution includes body force terms to represent the effect of the downstream OGV and splitter/strut. Similarly the OGV solution includes body force terms to account for the upstream fan rotor and the downstream strut/splitter, respectively. The numerical procedure solves the three-dimensional Reynolds averaged Navier-Stokes and energy equations using the four step Runge-Kutta scheme and is described by Adamczyk, et al. (Ref. 3). The standard two-equation k–ε model was used to calculate the turbulent eddy viscosity coefficient as described by Shabbir et al. (Refs. 4 and 5). Spalding's formula (Ref. 6) was used to set the wall boundary conditions for the mean flow equations as well as

the turbulence model. The inlet boundary conditions consisted of radial profiles of total pressure, total temperature, and radial and tangential flow angle which were deduced from the experimental data. The flow in the clearance gap was simulated using a model suggested by Kirtley et al. (Ref. 7) and treats the clearance flow as an orifice flow with no loss in mass, momentum, or energy. The effect of the vena contracta, which occurs in orifice flow is accounted for by using a discharge coefficient, which makes the effective tip clearance gap smaller than the actual clearance. Discharge coefficients of 0.5 to 1.0 are typically used (Ref. 8), however, a discharge coefficient of 1.0 is used for all results presented as advocated by Van Zante, et al., (Ref. 9). Typically 1 to 4 cells are used to define the clearance region. For this paper, the computational grids allow the number of cells in the clearance gap to vary with operating speed. In these simulations the tip clearance gap increased as the rotor speed decreased consistent with the thermal and mechanical stresses on the rotor and casing. The assessment of the change in clearances with rotor speed and inlet temperatures was provided by the experimental data. The APNASA solver expects a unique mesh for the rotor fan, OGV and strut, each of which shares a common axisymmetric grid as shown in Figure 2. The computational grids used for the present calculations were generated using TGS, a turbomachinery grid code developed by Beach (Ref. 10). The grids used by APNASA are sheared H-type in the blade-to-blade direction and incorporate a hyperbolic tangent stretching parameter to resolve the boundary layer and adequately define the flow regions. Similar stretching functions are chosen for the span-wise and chord-wise directions to enable adequate resolution of the blade leading and trailing edges and clearance gaps. The blade-to-blade stretching is relaxed to uniform spacing upstream and downstream of the blade rows since the flow is assumed to be periodic in those regions.

The grids used in the simulations had 80 cells in the radial direction, 50 cells in the circumferential direction with a total of 373 cells placed between the inlet and exit boundaries of which 60 were along the chord lines of each blade row (fan rotor, OGV, mid-frame strut).

Pretest Lessons Learned

Prior to the experiment, APNASA was run at 80 to 100 percent of rotor design speed. These pretest simulation results were compared to the experimental results of the fan stage characteristics at these speeds for the overall stage pressure ratio and adiabatic efficiency (see (Ref. 3)). In general, the simulations compared favorably with the data along the operating line both in terms of mass flow, pressure ratio, and to a lesser degree efficiency. However, a major concern at the time for the simulations was the inability of the code to predict the stall margin at 100 percent design speed. At 80 percent speed, the stall margin was well predicted. Analysis of the simulations as well as later comparisons with the experimental data led to the following issues:

1. The pretest simulation was run at the same bypass ratio as the data only along the operating line but at all other operating conditions along a speedline, the bypass ratio for the data and simulations were significantly different.
2. The measured rotor tip clearance was substantially lower than the clearance assumed by the simulations across the entire speed range. For example, the measured clearance at mid-chord of the rotor at 100 percent design speed was 0.30 mm (0.0012 in.) compared to the design intent of 0.51 mm (0.0020 in.) at design speed used in the computation.
3. The blade geometry was not properly hot-shape corrected resulting in the wrong blade geometry being simulated which can have a large effect on fan performance.

For the post-test assessment, the following adjustments were made to the grid and computational approach to circumvent these problems:

1. A mass flow boundary condition (Ref. 11) was used in the core flow which allowed the simulation to run with a boundary condition (in terms of bypass ratio) close to that at which the experimental data was acquired. This change allowed the bypass ratio of the simulation to better match the bypass ratio set in the experiment.
2. The simulation used the measured average tip clearance corresponding to each fan rotor speed. The average tip clearance was obtained by averaging the dynamic measurements of tip clearance for each blade made at the mid-chord region of the rotor blade at four different circumferential locations around the casing.
3. The blade geometry was corrected for rotational, temperature, and pressure loading corresponding to: 1) the blade cold shape, 2) hot shape corrected at 80 percent speed, and 3) hot shape geometry at 100 percent speed.

Post-Test simulations were performed with only the changes described above. This ensured that the conditions used in the simulations were similar to those of the experiment. The intent of these changes was to provide for a realistic assessment of the codes ability to predict the fan stage performance and operability.

Posttest APNASA Results and Comparison to Data

Post-Test simulations were performed at 100, 90, 80, 60, and 37 percent of fan rotor design speed. The hot shape corrected for 100 percent speed geometry was used for the 90 percent speed line simulations. The cold shape geometry was used for the 60 and 37 percent speed line simulations. The tip clearance over the rotor was assumed constant over the chord. The tip clearance values used in the computations are presented in Table 1 with the ratio of clearance gap to tip chord. Comparisons between the data and simulations were made in terms of pressure ratio and efficiency for the entire operating range at each of these speedlines. The pressure and temperature ratio were area-averaged and the adiabatic efficiency calculated based on the value of those two parameters. Tabulated results at choke, the operating point and near stall are presented with stall margin at the above fan speeds. The stall margin, SM, is defined as

$$SM = \frac{[PR/MF]_{NS}}{[PR/MF]_{OP}}$$

where PR is the pressure ratio, MF is the massflow, NS is the near stall point and OP is the operating point. The tip casing static pressure is also compared to data and is presented at the operating point for each of the fan speeds. Axisymmetric profiles are presented at the operating point and at the near stall point and compared to data at 100, 80, and 37 percent of the design speed. After these comparisons are made, an overall comparison is made of the data and the simulations, to the design intent only along the operating line at these same speeds.

TABLE 1.—SIMULATION ROTOR TIP CLEARANCE AT PERCENT SPEED

Speed (%)	mm	in.	Gap/chord (%)
100	0.30	0.012	0.26
90	.36	.014	.31
80	.41	.016	.35
60	.51	.020	.44
37	.66	.026	.57

Comparisons at 100 Percent Speed

Comparisons between the data and simulations at 100 percent design speed for the stage pressure ratio and adiabatic efficiency are shown in Figure 3. The experimental data is shown in red and the analysis in blue. The blue line represents the averaged results using the simulation results across the entire span and the blue symbols represent the averaged results using only the radial locations consistent with the radial locations that the measurements were acquired. This color scheme and symbol representation persists throughout this paper. It is evident from the results depicted in Figure 3 that the CFD does a credible job of predicting the pressure ratio and efficiency over the entire range of back-pressures and not just at the operating point for 100 percent speed. A more quantitative comparison is provided in Table 2. The parameters of corrected mass flow, pressure ratio (PR), temperature ratio (TR), adiabatic efficiency, and stall margin are provided for the data and simulation for points along the speedline. These points are choke, the operating line, and near stall. The only valid comparison for the choke flow condition is to compare the mass flow for the data to that of the simulation because the fan stage characteristic is essentially vertical. No attempt was made in the simulation to match the

data at the lowest pressure ratio. However, it was felt important to report the maximum flow condition and compare to the data, especially at high rotational speeds. If there is good agreement in the choked flow between the data and the simulation, then there is a high degree of confidence that the geometry is being accurately modeled in the simulations. It is also evident that the agreement between the simulation and the data is much better at the operating line than at the choked flow and near stall conditions where the likelihood of separated and unsteady flow effects are much higher.

TABLE 2.—QUANTITATIVE COMPARISON OF SIMULATION
RESULTS TO DATA AT 100 PERCENT SPEED

	Speed (%)	100		
	Flow	Choke	Op	NS
Data	Mass flow	37.459	37.318	34.827
APNASA	(kg/s)	37.432	37.328	34.645
Data	Pressure		2.518	2.571
APNASA	ratio (PR)		2.486	2.557
Data	Temperature		1.354	1.383
APNASA	ratio (TR)		1.342	1.37
Data	Efficiency		0.844	0.799
APNASA			0.865	0.828
Data	Stall margin		9.41	
APNASA	(%)		10.82	

Figure 3 indicates that the simulation is producing higher efficiencies than the data. Further comparisons between the data and simulation indicates that the fan rotor static pressure rise at the tip is being over-predicted by the simulation (see Fig. 4) which is indicative of not accurately capturing the fan endwall flow characteristics which could be due to not modeling the non-uniform distribution of the fan tip clearance from leading edge to trailing edge. It should be noted that in the experiment, the rotor tip rubbed in near the trailing edge at 100 percent speed.

Profiles of total pressure and efficiency behind the OGV at the operating point and near stall are shown in Figure 5. At the operating line, the simulation total pressure in Figure 5(a) exhibits a lower level of total pressure than the data but with a consistent shape. There also appears to be a higher level of total pressure near the hub in the simulation that is not seen in the data. The simulation efficiency overall in Figure 5(b) is higher than the data which was pointed out earlier but the shape follows the general trend of the data. Since the efficiency matches so well near the tip and the total pressure ratio is lower, the simulation overpredicts the measured total temperature.

At near stall in Figure 5(c), the total pressure level below midspan from the simulation is lower than experiment and is overpredicted in the upper 50 percent span. Similarly in

Figure 5(d), the efficiency is underpredicted near the hub and overpredicted from 40 percent span outward. The wiggles in the profile below midspan indicate weak (separated) flow near the hub that is not evident in the experimental data.
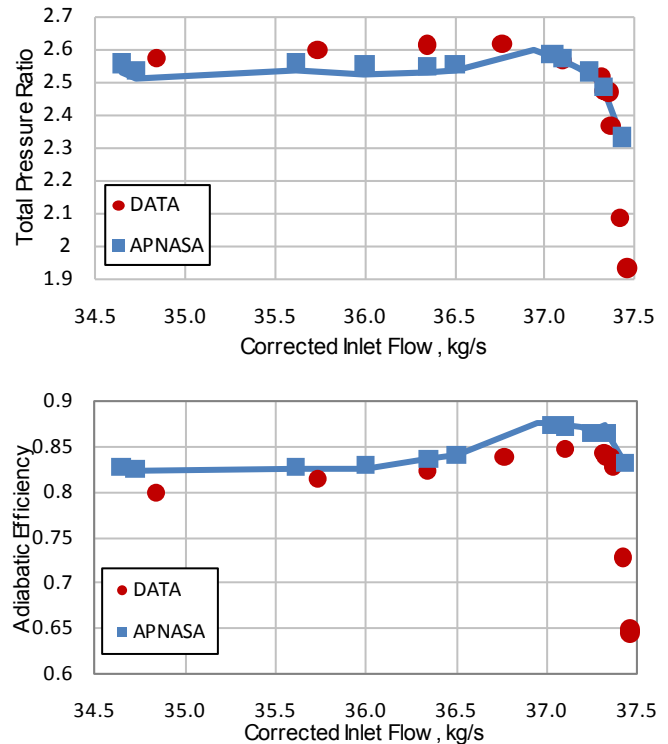

Figure 3.—Stage pressure ratio and adiabatic efficiency versus corrected inlet flow at 100 percent speed.
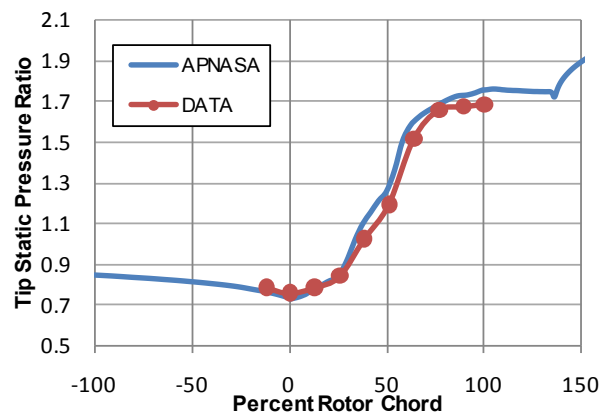

Figure 4.—Comparison of casing static pressure with data at 100 percent speed at the operating point.
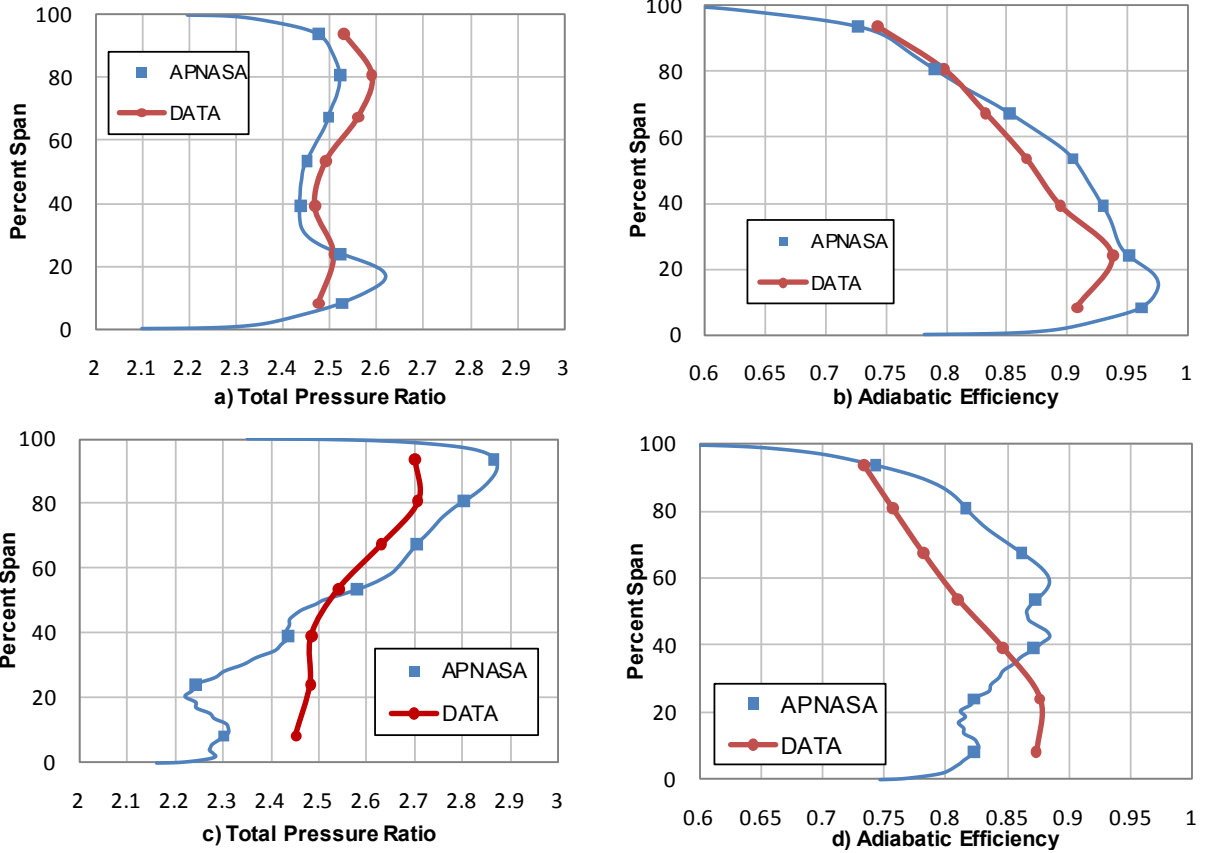
Figure 5.—Profiles of total pressure ratio and adiabatic efficiency aft of the OGV at the operating point ((a) and (b)) and near stall ((c) and (d)) at 100 percent speed.
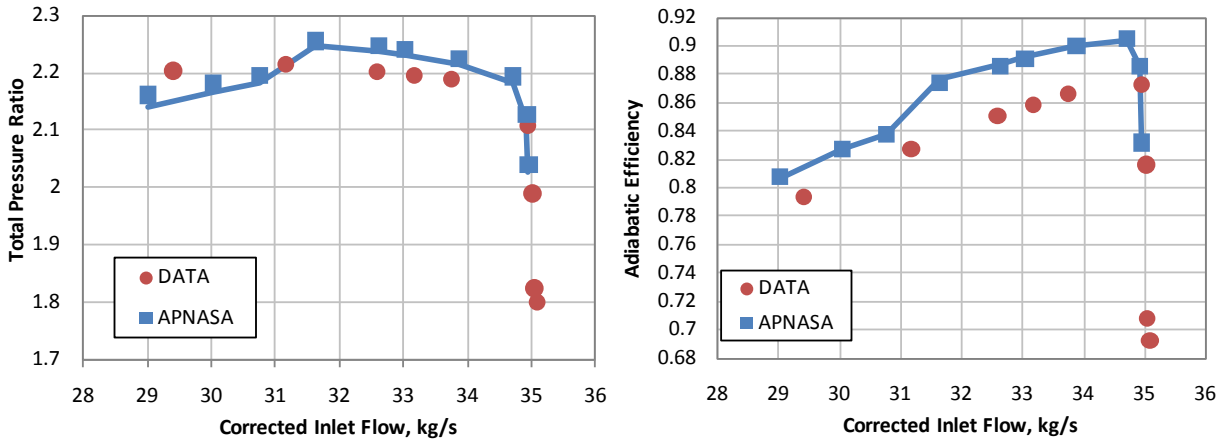

Figure 6.—Stage pressure ratio and adiabatic efficiency versus corrected inlet flow at 90 percent speed.

Comparisons at 90 Percent Speed

Comparisons between the data and simulations at 90 percent speed for the stage pressure ratio and adiabatic efficiency are shown in Figure 6. The simulation results at 90 percent speed, similar to those at 100 percent speed, show good agreement across the operating range. Pressure ratio is well predicted at the operating line but the efficiency is still over-predicted by about 3 points at the operating point similar to the 100 percent speed results. Tabulated results for choke, the operating point and near stall are found in Table 3. Stall margin from the simulation was slightly lower than determined from the data.

TABLE 3.—QUANTITATIVE COMPARISON OF SIMULATION
RESULTS VERSUS DATA AT 90 PERCENT SPEED

	Speed (%)	90		
	Flow	Choke	Op	NS
Data	Mass flow	35.084	33.178	29.410
APNASA	(kg/s)	34.956	33.035	29.009
Data	Pressure		2.195	2.202
APNASA	ratio (PR)		2.24	2.161
Data	Temperature		1.292	1.316
APNASA	ratio (TR)		1.29	1.304
Data	Efficiency		0.858	0.793
APNASA			0.89	0.808
Data	Stall margin	13.17		
APNASA	(%)	9.86		

Comparisons at 80 Percent Speed

Comparisons between the data and simulations at 80 percent design speed for the stage pressure ratio and adiabatic efficiency are shown in Figure 7 with the quantitative comparisons tabulated in Table 4. At this speed, the agreement in total pressure is very good and differs from the data by less than 1 percent even at near stall. The efficiency calculation is overpredicted by less than 3 points at the operating point and slightly more than 3 points at near stall. The stall margin from the simulation agrees very well with the data. Figure 8 shows a comparison of the casing static pressure between the simulation and the data at the operating line. It shows that the pressure at the casing from the simulation agrees very well with the data over the rotor chord indicating that the shock location between the data and the simulation are practically identical. Profiles of total pressure ratio and adiabatic efficiency on the operating line, (a) and (b), and near stall, (c) and (d) are shown in Figure 9. Similar to the 100 percent speed profiles, the simulation profiles for total pressure ratio and adiabatic efficiency agree quite well with data at the operating line. Near the hub, however, the simulation profile indicates a stronger hub flow than the experiment. This stronger hub flow persists to near stall as indicated by the level of higher total pressure near the hub.

TABLE 4.—QUANTITATIVE COMPARISON OF SIMULATION
RESULTS VERSUS DATA AT 80 PERCENT SPEED

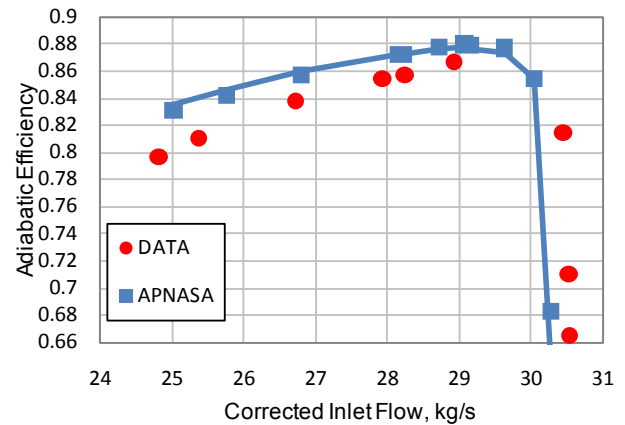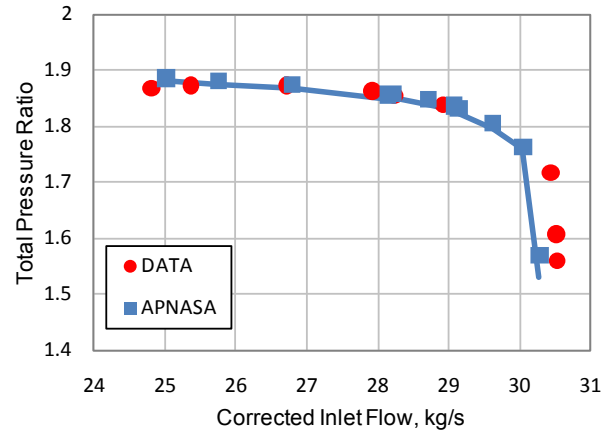|	Speed (%)	80		
	Flow	Choke	Op	NS
Data	Mass flow	30.529	29.233	24.810
APNASA	(kg/s)	30.281	28.206	25.014
Data	Pressure		1.855	1.869
APNASA	ratio (PR)		1.858	1.886
Data	Temperature		1.224	1.244
APNASA	ratio (TR)		1.222	1.239
Data	Efficiency		0.857	0.797
APNASA			0.872	0.831
Data	Stall margin	14.66		
APNASA	(%)	14.46		

Figure 7.—Stage pressure ratio and adiabatic efficiency versus corrected inlet flow at 80 percent speed.
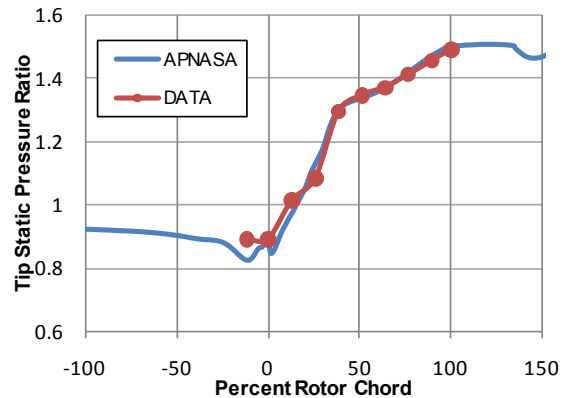

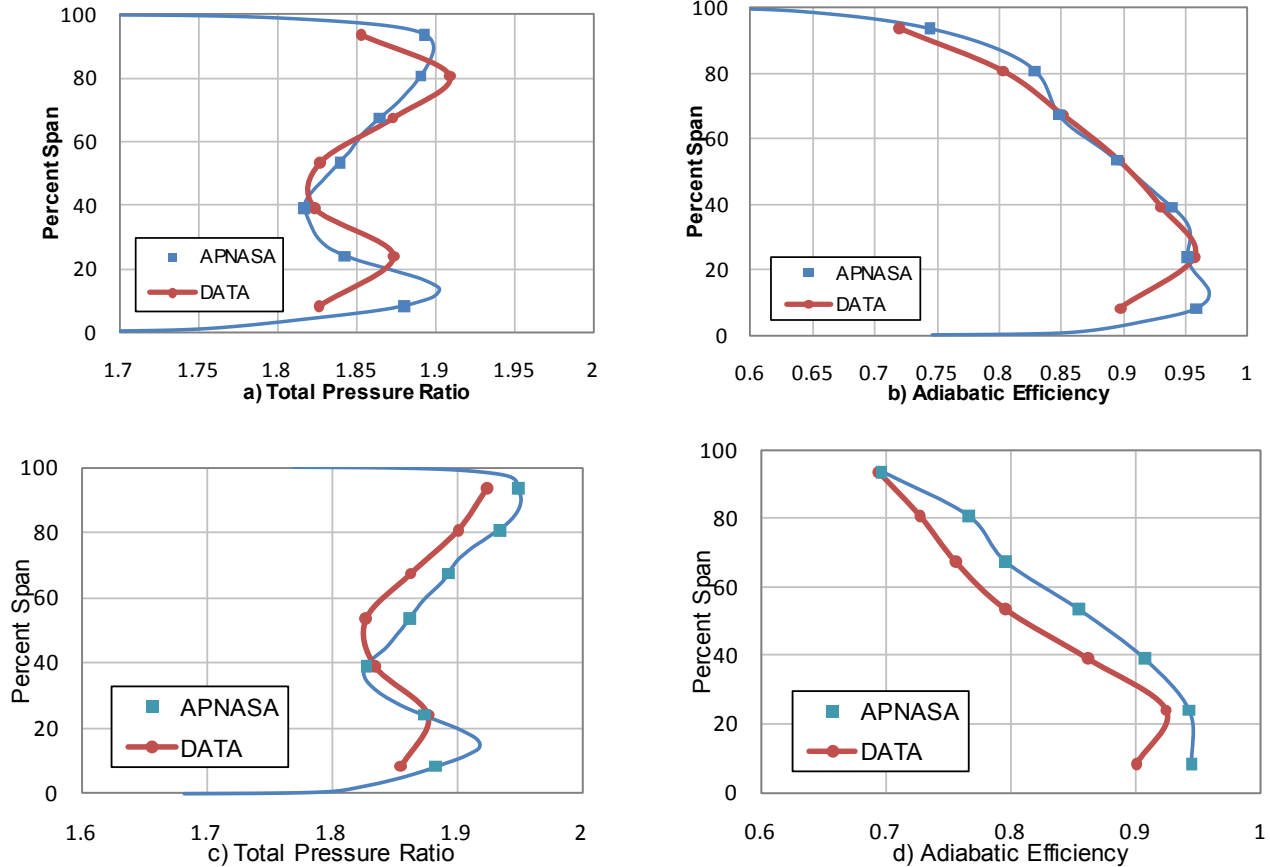Figure 8.—Comparison of casing static pressure with data at 80 percent speed at operating point.

Figure 9.—Profiles of total pressure ratio and adiabatic efficiency aft of the OGV at the operating point ((a) and (b)) and near stall ((c) and (d)) at 80 percent speed.
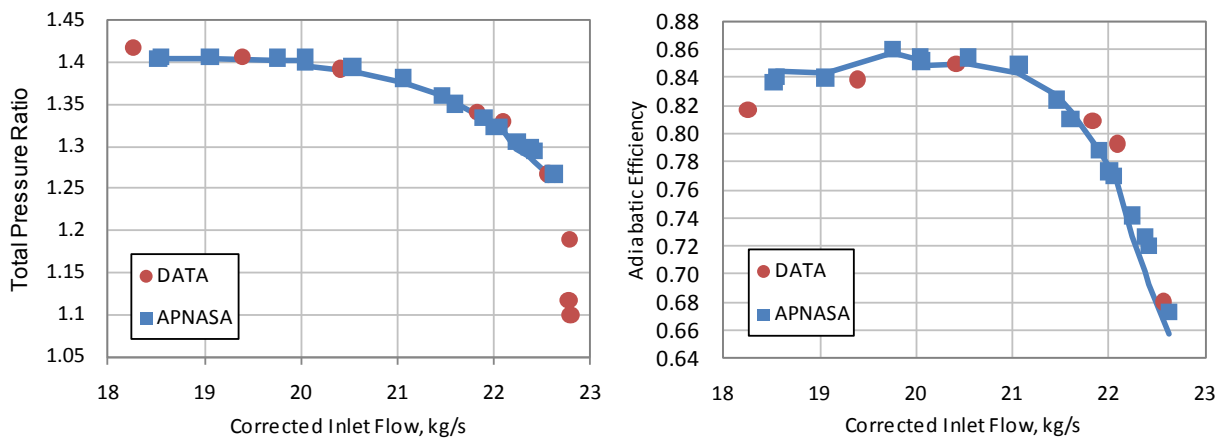

Figure 10.—Stage pressure ratio and adiabatic efficiency versus corrected inlet flow at 60 percent speed.

Comparisons at 60 Percent Speed

Comparisons between the data and simulations at 60 percent design speed for the stage pressure ratio and adiabatic efficiency are shown in Figure 10 with the results tabulated in Table 5. At this speed, the agreement in total pressure is very good and differs from the data by less than 1 percent even at near stall. The efficiency calculation is again overpredicted by less than 3 points but is now nearly within the uncertainty measurements of the data. The stall margin from the simulation is 3.31 points lower than the data.

TABLE 5.—QUANTITATIVE COMPARISON OF SIMULATION
RESULTS VERSUS DATA AT 60 PERCENT SPEED.

	Speed (%)	60		
	Flow	Choke	Op	NS
Data	Mass flow	22.800	22.091	18.255
APNASA	(kg/s)	22.623	22.051	18.518
Data	Pressure		1.329	1.417
APNASA	ratio (PR)		1.324	1.404
Data	Temperature		1.107	1.128
APNASA	ratio (TR)		1.108	1.122
Data	Efficiency		0.793	0.817
APNASA			0.77	0.836
Data	Stall margin	29.03		
APNASA	(%)	26.27		

Comparisons at 37 Percent Speed

Comparisons between the data and simulations at 37 percent design speed for the stage pressure ratio and adiabatic efficiency are shown in Figure 11 with the results tabulated in Table 6. At this speed, the agreement in total pressure is very good over most of the speedline, but is underpredicted at flow less than 12 kg/s and more than 16 kg/s. The efficiency, however, tracks the data very well with a slight overprediction near stall. The stall margin from the simulation is a little more than 2.5 points lower than the data. Figure 12 shows a comparison of the casing static pressure between the simulation and the data at the operating line. The pressure at the casing from the simulation agrees very well with the data over the over front half of the rotor chord and higher than the data aft of mid-chord. This over-prediction may be due to the tighter measured clearance in the back end of the rotor which was reported but not simulated. Profiles of stage total pressure ratio and adiabatic efficiency on the operating line and near stall are shown in Figure 13. The simulation profiles for total pressure ratio agree quite well with data at the operating line above 40 percent span. Near the hub, the simulation shows a rather large total pressure deficit up to about 20 percent which is not seen in the data. At near stall, the simulation exhibits a similar profile to the data but at a slightly lower level. The efficiency calculation from the data has a large degree of uncertainty because the total temperature rise at 37 percent design speed is quite low. See (Ref. 3).

TABLE 6.—QUANTITATIVE COMPARISON OF SIMULATION
RESULTS VERSUS DATA AT 37 PERCENT SPEED

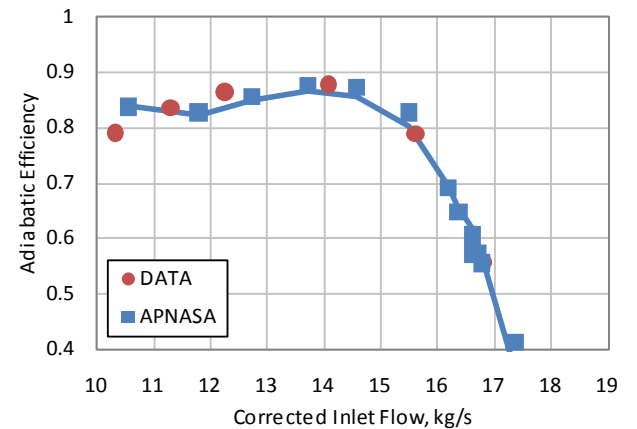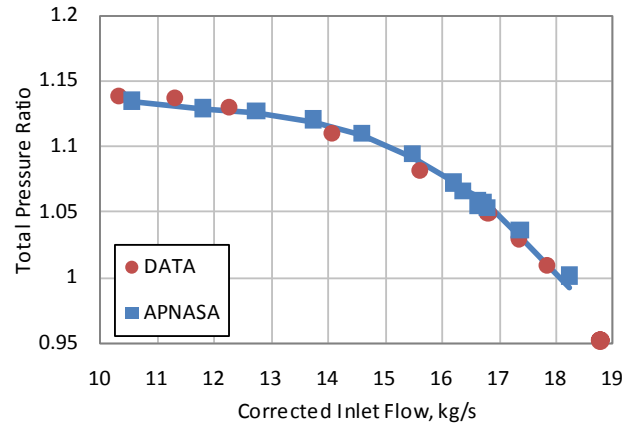|	Speed (%)	37		
	Flow	Choke	Op	NS
Data	Mass flow	18.767	17.349	13.311
APNASA	(kg/s)	18.236	17.355	10.552
Data	Pressure		1.03	1.139
APNASA	ratio (PR)		1.025	1.135
Data	Temperature		1.023	1.048
APNASA	ratio (TR)		1.025	1.044
Data	Efficiency		0.372	0.791
APNASA			0.412	0.838
Data	Stall margin	86.06		
APNASA	(%)	82.11		

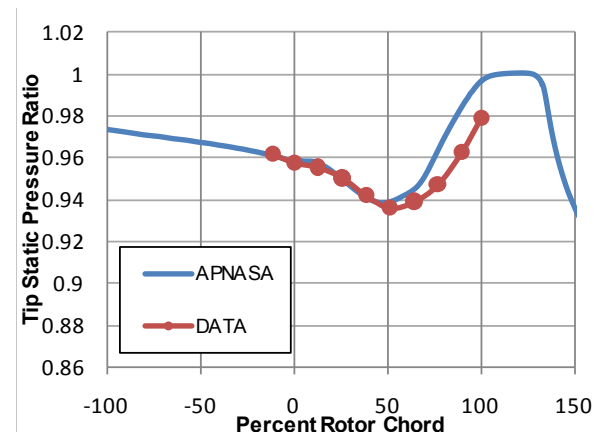Figure 11.—Stage pressure ratio and adiabatic efficiency versus corrected inlet flow at 37 percent speed.

Figure 12.—Comparison of casing static pressure with data at operating point at 37 percent speed.
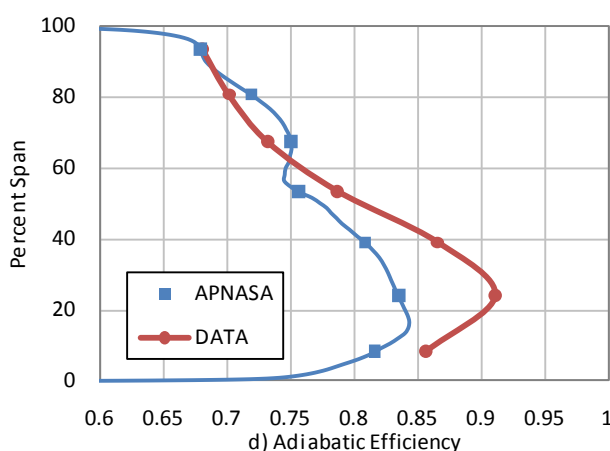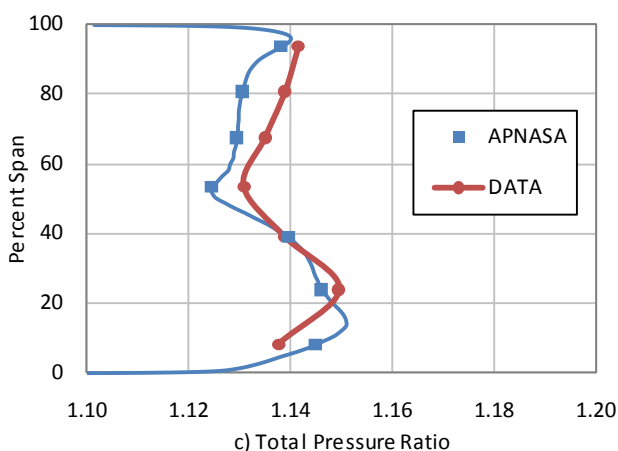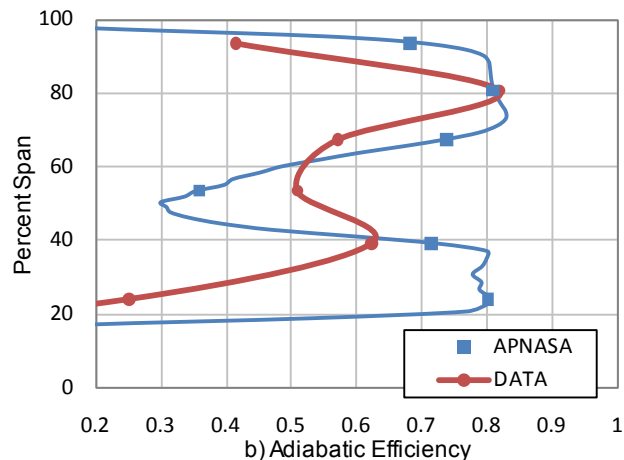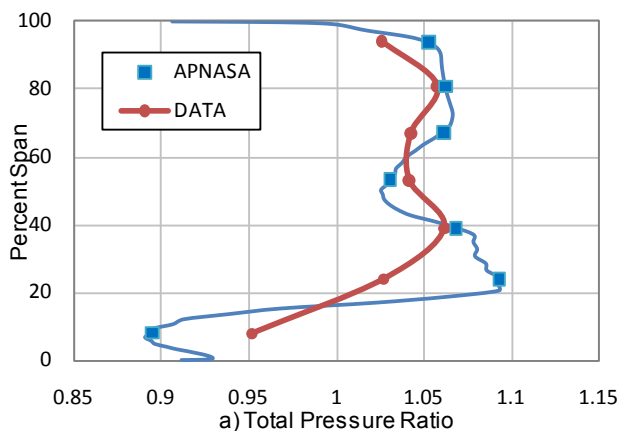
Figure 13.—Profiles of total pressure ratio and adiabatic efficiency aft of the OGV for the operating point ((a) and (b)) and near stall ((c) and (d)) at 37 percent speed.

Overall Comparisons Along the Design Operating Line

Some overall parameters were compared to design intent along the operating line. Figure 14 plots the total pressure ratio along the entire operating line from 37 to 100 percent fan speed for the results obtained from the design intent, i.e., GE's design cycle deck, and compared to the experimental data and APNASA.

The percent rotational speed of the fan is plotted along the abscissa, with the stage total pressure ratio plotted along the ordinate. APNASA tracks the data (red circles) very well, however, note how well the design intent also tracks the data. Figure 15 compares the corrected inlet mass flow with percent speed along the operating line. Again, it is difficult to distinguish between APNASA and the experimental data on this scale. The symbol for the data has been exaggerated for clarity. Figure 16 compares adiabatic efficiency with percent design speed also along the operating line. As was mentioned earlier in the comparisons, APNASA overpredicts the efficiency. As the percent speed drops to below 80 percent, the
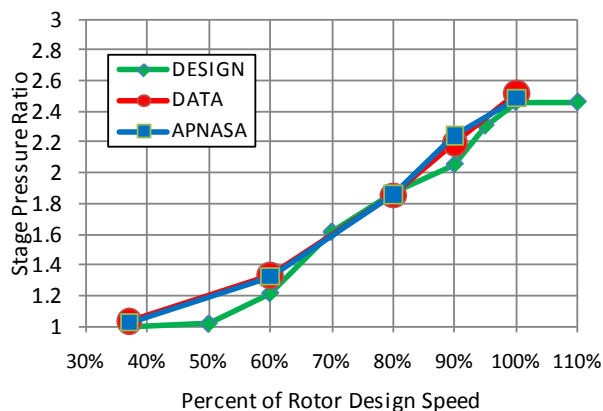

Figure 14.—Comparison of stage pressure ratio versus percent speed along the operating line.

difference in efficiency decreases. This overprediction of efficiency has been shown reported in the literature but the cause for this is not known. Figure 17 compares stall margin versus percent design speed. Again, the symbol for the experimental data has been exaggerated for clarity. Overall, APNASA was able to track the stall margin computed from the experimental data quite well which points to the tools suitability to analyze similar concepts.
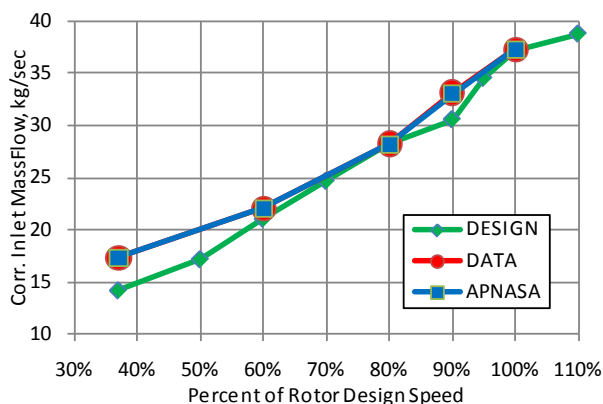

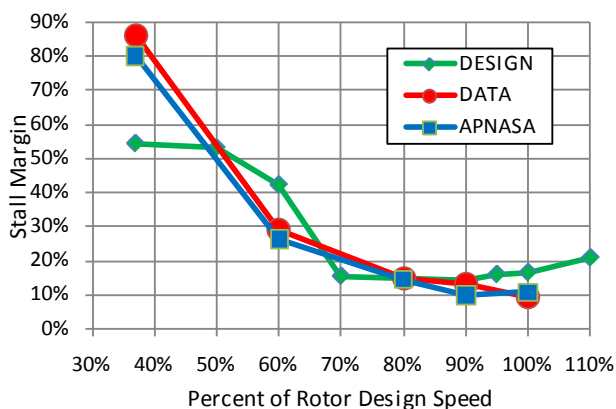Figure 15.—Comparison of corrected inlet mass flow versus percent speed along the operating line.

Figure 16.—Comparison of adiabatic efficiency versus percent design speed along the operating line.
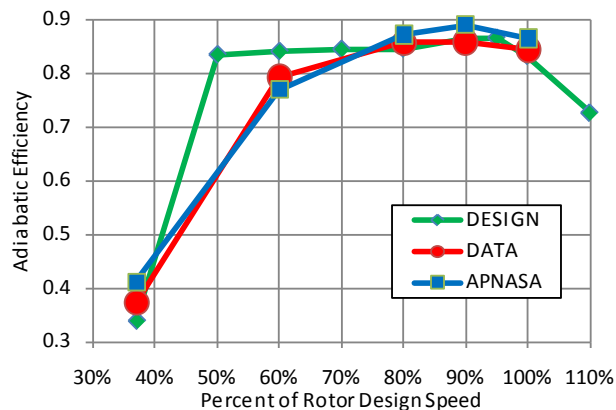

Figure 17.—Comparison of stall margin versus percent design speed.

Summary and Concluding Remarks

The RTA fan rig was simulated by APNASA for a wide operating range of speeds (37 to 100 percent) following some lessons learned from a pretest prediction of the same geometry. These lessons included the importance of having the correct hot shape, setting the proper tip clearance for the rotor simulations and understanding what boundary conditions are necessary to obtain good simulation results. These simulations were compared to experimental data taken at the NASA Glenn Research Center in their High Speed Compressor facility. The comparisons showed that the stage pressure ratio compared quite well to the data with the efficiency overpredicted by less than 3 points. Profiles of total pressure ratio and adiabatic efficiency were compared to data at both the operating line and near stall. The simulation profiles, for the most part, compared well to the data. In the near stall case at design speed, APNASA predicted a weaker hub flow than the data which will be looked at more carefully. APNASA was able to compute the flow at all the range of speeds required as well as obtain a fan stall margin that compared quite well with the data. This work shows that APNASA can be used to help design and analyze similar future fan stage concepts.

References

1. Adamczyk, J.J., Celestina, M.L., Beach, T.A. and Barnet, M., "Simulation of Three-dimensional Viscous Flow Within a Multistage Turbine," Trans. ASME, 112, pp. 370–376.
2. Mielke M., Clark, D.S., and Wood, P., "RTA/GE57 Subscale Fan Rig, Final Report - Aero & Aeromechanical," NASA/CR—2010-215815.
3. Suder, K., Prahst, P., and Thorp, S., "Results of an Advanced Fan Stage Operating Over a Wide Range of Speed and Bypass Ratio—Part I: Fan Stage Design and Experimental Results," ASME, 2010. GT2010-22825.
4. Shabbir, A., Zhu, J., and Celestina, M.L. "Assessment of the Three-Dimensional Models in a Compressor Rotor," ASME, 1996. ASME Paper No. 96–GT–198.
5. Shabbir, A. and Turner, M.G., "A Wall Function for Calculating the Skin Friction with Surface Roughness," ASME, 2004. Paper GT2004–53908.
6. Spalding, D.B., "A Single Formula for the Law of the Wall," 1961, J. Appl Mech., pp. 455–458.
7. Kirtley, K.R., Beach, T.A., and Adamczyk, J.J. Numerical Analysis of Secondary Flow in a Two-Stage Turbine. AIAA, 1990, AIAA–90–2356.
8. Shabbir, A., Adamczyk, J.J., Strazisar, A.J., and Celestina, M.L., "The Effect of Hub Leakage Flow on Two High-Speed Axial Flow Compressor Rotors," ASME, 1997. Paper 97–GT–346.
9. VanZante, D., Strazisar, A., Wood, J., Hathaway, M., and Okiishi, T., "Recommendations for Achieving Accurate Numerical Simulation of Tip Clearance Flows in Transonic Compressor Rotors," ASME, Oct. 2000, J. of Turbomachinery, Vol. 122, p. 733.
10. Adamczyk, J.J. Private Communication.
11. Beach, T. Private Communication.

1. REPORT DATE (DD-MM-YYYY) 01-10-2010	2. REPORT TYPE Technical Memorandum	3. DATES COVERED (From - To)

4. TITLE AND SUBTITLE
Results of an Advanced Fan Stage Operating Over a Wide Range of Speed and Bypass Ratio
Part 2: Comparison of CFD and Experimental Results

5a. CONTRACT NUMBER

5b. GRANT NUMBER

5c. PROGRAM ELEMENT NUMBER

6. AUTHOR(S)
Celestina, Mark, L.; Suder, Kenneth, L.; Kulkarni, Sameer

5d. PROJECT NUMBER

5e. TASK NUMBER

5f. WORK UNIT NUMBER
WBS 599489.02.07.03.07

7. PERFORMING ORGANIZATION NAME(S) AND ADDRESS(ES)
National Aeronautics and Space Administration
John H. Glenn Research Center at Lewis Field
Cleveland, Ohio 44135-3191

8. PERFORMING ORGANIZATION REPORT NUMBER
E-17395-2

9. SPONSORING/MONITORING AGENCY NAME(S) AND ADDRESS(ES)
National Aeronautics and Space Administration
Washington, DC 20546-0001

10. SPONSORING/MONITOR'S ACRONYM(S)
NASA

11. SPONSORING/MONITORING REPORT NUMBER
NASA/TM-2010-216769-PART2

12. DISTRIBUTION/AVAILABILITY STATEMENT
Unclassified-Unlimited
Subject Category: 02
Available electronically at http://gltrs.grc.nasa.gov
This publication is available from the NASA Center for AeroSpace Information, 443-757-5802

13. SUPPLEMENTARY NOTES

14. ABSTRACT
NASA and GE teamed to design and build a 57 percent engine scaled fan stage for a Mach 4 variable cycle turbofan/ramjet engine for access to space with multipoint operations. This fan stage was tested in NASA's transonic compressor facility. The objectives of this test were to assess the aerodynamic and aero mechanic performance and operability characteristics of the fan stage over the entire range of engine operation including: 1) sea level static take-off; 2) transition over large swings in fan bypass ratio; 3) transition from turbofan to ramjet; and 4) fan wind-milling operation at high Mach flight conditions. This paper will focus on an assessment of APNASA, a multistage turbomachinery analysis code developed by NASA, to predict the fan stage performance and operability over a wide range of speeds (37 to 100 percent) and bypass ratios.

15. SUBJECT TERMS
Fan stage; Compressor rotor

16. SECURITY CLASSIFICATION OF:			17. LIMITATION OF ABSTRACT	18. NUMBER OF PAGES	19a. NAME OF RESPONSIBLE PERSON STI Help Desk (email:help@sti.nasa.gov)
a. REPORT U	b. ABSTRACT U	c. THIS PAGE U	UU	16	19b. TELEPHONE NUMBER (include area code) 443-757-5802